

ENGINEERING PROGRESS at the UNIVERSITY OF FLORIDA

Vol. XV, No. 9

September, 1961



Technical Paper No. 206

Cohesion after Non-Hydrostatic Consolidation

by

John H. Schmertmann
and
John R. Hall, Jr.

Reprinted from the *Journal of the Soil Mechanics and
Foundations Division, ASCE, August, 1961.*

Published monthly by the

FLORIDA ENGINEERING AND INDUSTRIAL EXPERIMENT STATION

COLLEGE OF ENGINEERING • UNIVERSITY OF FLORIDA • GAINESVILLE

Entered as second-class matter at the Post Office at Gainesville, Florida

Journal of the
SOIL MECHANICS AND FOUNDATIONS DIVISION
Proceedings of the American Society of Civil Engineers

COHESION AFTER NON-HYDROSTATIC CONSOLIDATION

By John H. Schmertmann,¹ A. M. ASCE, and John R. Hall, Jr.,² A. M. ASCE

SYNOPSIS

A study was made to determine the effect of non-hydrostatic consolidation on the cohesion and friction in two saturated clays using the CFS-test procedure. The results showed that cohesion is unaffected by non-hydrostatic consolidation. The value of friction at zero CFS-test strain is increased by non-hydrostatic consolidation but the variation of friction with strain is the same as in a hydrostatically consolidated sample. In addition a time transfer of cohesion to friction was observed.

INTRODUCTION

Notation.—The letter symbols adopted for use in this paper are defined where they first appear, in the illustration or in the text, and are arranged alphabetically, for convenience or reference, in the Appendix.

Review of CFS-test.—A previous paper³ reported the first published results of the basic research on the components of soil strength being performed in Soil Mechanics Research Laboratory of the University of Florida. This reference reports the development of a triaxial compression test, termed the CFS (an abbreviation of cohesion-friction-strain)-test, designed to permit the com-

Note.—Discussion open until January 1, 1962. To extend the closing date one month, a written request must be filed with the Executive Secretary, ASCE. This paper is part of the copyrighted Journal of the Soil Mechanics and Foundations Division, Proceedings of the American Society of Civil Engineers, Vol. 87, No. SM 4, August, 1961.

¹ Asst. Prof. of Civ. Engrg., Univ. of Florida, Gainesville, Fla.

² Graduate Asst., Civ. Engrg. Dept., Univ. of Florida, Gainesville, Fla.

³ "An Experimental Study of the Development of Cohesion and Friction with Axial Strain in Saturated Cohesive Soils," by J. H. Schmertmann and J. O. Osterberg, June 1960 Research Conf. on Shear Strength of Cohesive Soils, ASCE, July, 1961.

putation of cohesion and friction at strain intervals during compression and thereby establish curves of the variation of cohesion and friction with strain. Since an understanding of the definitions used for cohesion and friction and the techniques of the CFS-test are necessary in order to follow the work reported herein, they are briefly reviewed in this introduction:

The angle of internal friction ϕ_ϵ at any strain is the angle for which the tangent is the ratio of the change in shear stress to the change in normal effective stress occurring on the plane of Mohr envelope tangency at that strain, during a stress change occurring without significant change in soil structure.

The cohesion c_ϵ of a soil, at any strain ϵ , is the shear stress developed on the plane of Mohr envelope tangency at that strain, if the effective stress on that plane could be reduced to zero with proportionally the same change in soil structure as occurs in the determination of ϕ_ϵ .

For saturated soils, the effective stress at a point is defined as the total stress less the pore water pressure measured by a piezometer at that point. The plane of Mohr envelope tangency is the plane of maximum stress obliquity for the frictional component of strength. The expression "without significant change in soil structure" is, as of 1961, interpreted to be a void ratio change of less than 1% in the same soil, caused solely by a change in pore pressure.

From the foregoing, one may see that the cohesion and friction definitions used herein have a physical significance which one can "feel" and work with in the laboratory. The expressions "cohesion" and "friction" are retained herein for continuity with the previous work.³ However, other expressions for these components, such as "pore pressure insensitive" and "pore pressure sensitive," may eventually be preferred. There is no claim that these are basic mechanical properties of a soil. The definitions were chosen with the hope that they will eventually prove useful in engineering application and thereby justify their existence. The writers are optimistic that this is the case. This work presents only part of the results from a research program active at the University of Florida, under the direction of the senior writer, and therefore represents only a part of the experimental evidence that will eventually be presented for the evaluation of the engineering significance of the CFS-test definitions and procedures.

Fig. 1 helps to explain the CFS-test technique. An axial deviator stress, σ_a , is imposed on a soil specimen in the triaxial chamber by subjecting the specimen to a constant rate of compressive strain. During this strain the pore water pressure is externally controlled to maintain a constant value of major principal effective stress, $\bar{\sigma}_1$, on any horizontal plane such as 1-1 in Fig. 1 (a). The control is by periodic manual adjustments of pore water pressure, u , to maintain a value of

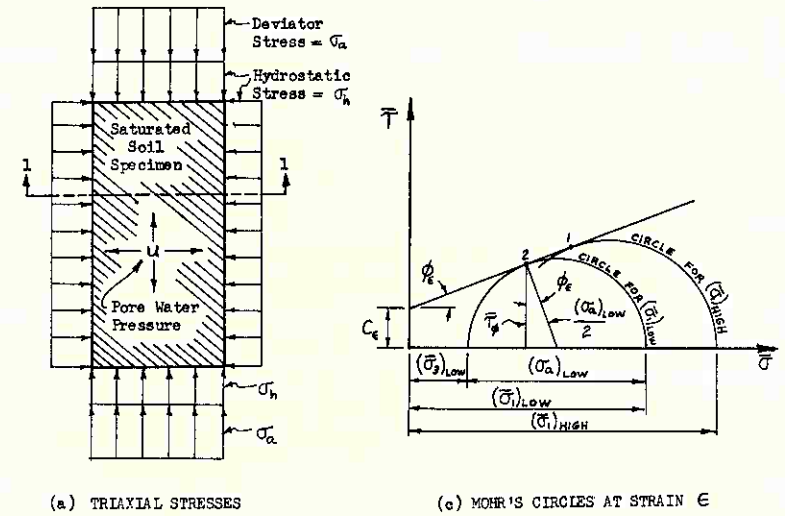
$$u = \sigma_a + (\sigma_h - \bar{\sigma}_1) \dots \dots \dots (1)$$

in which σ_h is the constant cell pressure and $\bar{\sigma}_1$ is held constant at a pre-selected value. Thus,

$$u = \sigma_a + (\text{a constant}) \dots \dots \dots (2)$$

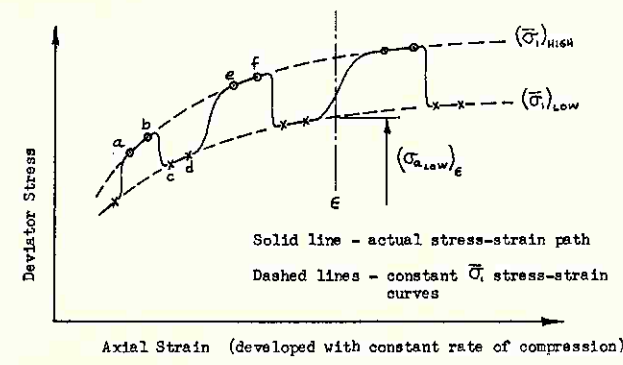
One of the pre-selected $\bar{\sigma}_1$ values is the $(\bar{\sigma}_1)_{\text{high}}$ indicated in Fig. 1(b). Two successive deviator stress-strain data points are obtained at this $(\bar{\sigma}_1)_{\text{high}}$, as represented by points a and b. The pore pressure is then increased to reduce $\bar{\sigma}_1$ to the pre-selected value of $(\bar{\sigma}_1)_{\text{low}}$. In the work reported herein the $(\bar{\sigma}_1)_{\text{high}}$ value was 95% $(\bar{\sigma}_1)_c$ imposed during consolidation, and the $(\bar{\sigma}_1)_{\text{low}}$ was 75% $(\bar{\sigma}_1)_c$. The increased pore pressure reduces the frictional component of

strength and thus reduces the deviator stress the specimen can support at that strain. Because the test is strain controlled, the result is a measured reduction in deviator stress instead of an increase in strain. After sufficient time for $\bar{\sigma}_1$ equilibrium at the lower value, two additional stress-strain data points



(a) TRIAXIAL STRESSES

(c) MOHR'S CIRCLES AT STRAIN ϵ



(b) STRESS-STRAIN CURVES

FIG. 1.—TECHNIQUE OF CFS-TEST

are obtained, as represented by points c and d. The pore pressure is then reduced to raise $\bar{\sigma}_1$ to the $(\bar{\sigma}_1)_{\text{high}}$ value which results in increased friction and measured deviator stress: Points e and f are obtained to define two stress-strain curves, one for each $\bar{\sigma}_1$ as shown by the dashed lines in Fig. 1 (b).

At any value of strain, such as ϵ in Fig. 1 (b), a Mohr circle can be drawn representing the stress conditions for the specimen at each $\bar{\sigma}_1$ value. The two circles obtained are shown in Fig. 1 (c). The angle made by the tangent line 1-2 with the $\bar{\sigma}$ axis is ϕ_ϵ , which is then used in Eq. 3 to obtain c_ϵ . Eq. 3 is derived from the relationships shown in Fig. 1 (c):

$$c_\epsilon = \frac{\frac{\sigma_a}{2} - \sin \phi_\epsilon \left(\frac{\sigma_a}{2} + \bar{\sigma}_3 \right)}{\cos \phi_\epsilon} \dots \dots \dots (3)$$

The values of ϕ_ϵ and c_ϵ thus obtained are plotted against strain, yielding a curve of cohesion-friction-strain behavior for the soil specimen tested.

Purpose.—In any field situation the soil is actually consolidated under non-hydrostatic stress conditions rather than the convenient hydrostatic consolidation usually employed in the laboratory triaxial test. It is therefore important to know if non-hydrostatic consolidation results in materially different subse-

TABLE 1.—SUMMARY OF RESEARCH PROGRAM

Test Series (1)	Soil Type (2)	Number of Tests (3)	$(\bar{\sigma}_1)_c$ (4) ^a	$\left(\frac{\bar{\sigma}_1}{\bar{\sigma}_3}\right)_c$ Ratio Used (5) ^a	Consolidation Method (6)
I	Kaolinite	4	1.80 kg/cm ²	1.0, 1.2, 1.4, 1.6	Standard (see procedures)
II	Kaolinite	4	3.65 "	1.0, 1.2, 1.4, 1.6	Standard
III	Boston Blue Clay	4	3.65 "	1.0, 1.2, 1.4, 1.6	Standard
IV	Kaolinite	1	5.73 "	1.6	Standard, but increased time in secondary.
		2	3.65 "	1.6	
V	Kaolinite	2	3.65 "	1.6	1. σ_1/σ_3 kept constant during loading 2. $(\sigma_1 - \sigma_3)$ added after consolidation to $(\bar{\sigma}_3)_c$

^a Approximate.

quent strength behavior when compared to hydrostatic consolidation. All previous CFS-test work followed hydrostatic consolidation.

The writers were especially interested in further study of the cohesion component of strength. One result of the previous work³ was that the value of maximum principal effective stress, $\bar{\sigma}_1$, seemed much more important than soil structure in determining cohesion behavior. However, the possible importance of anisotropic structure was not studied. Such a study was one of the purposes of the work reported herein.

If cohesion is anisotropic due to anisotropy of soil structure, then the work by A. Casagrande, F. ASCE, and N. Carrill indicates⁴ that for a constant value of maximum cohesion, and a constant position of the plane of maximum cohesion, the cohesion developed on the potential failure planes should vary measurably with significant variations in the degree of structural anisotropy. In this study,

⁴ "Shear Failure of Anisotropic Materials," by A. Casagrande and N. Carrillo, *Contributions to Soil Mechanics 1941-1953*, Boston Soc. of Civ. Engrs., p. 122.

TABLE 2.—SUMMARY OF TEST CONDITIONS

Series (1)	Test Number (2)	Sample Type Number (3)	Test Date, 1959-60 (4)	$(\bar{\sigma}_1)_c$ (5)	$\left(\frac{\bar{\sigma}_1}{\bar{\sigma}_3}\right)_c$ (6)	Axial Consolidation Compression, h_i in centimeters (7)	Computed Values			
							Before consolidation		After CFS-test	
							e (8)	S% (9)	e (10)	S% (11)
I	H-17	DWEPK 795	1-21	1.80	1.00	0.258	1.059	100.5	0.958	101.2
	H-18	" 793	1-24	1.83	1.22	0.378	1.057	100.9	0.948	100.2
	H-19	" 792	1-26	1.84	1.42	0.469	1.057	100.9	0.945	100.8
	H-21	" 790	2-14	1.83	1.59	0.57	1.057	100.6	0.945	100.3
II	H-13	DWEPK 799	12-12	3.65	1.00	0.399	1.064	99.8	0.899	99.6
	H-14	" 798	1-10	3.81	1.21	0.546	1.064	99.6	0.883	100.0
	H-15	" 797	1-13	3.69	1.39	0.686	1.053	100.6	0.887	99.7
	H-16	" 796	1-19	3.56	1.58	0.818	1.055	100.6	0.901	100.8
III	H-22	BBC 539	2-20	3.65	1.00	0.233	0.744	99.8	0.645	100.0
	H-23	" 538	2-23	3.66	1.20	0.35	0.758	97.6	0.651	98.2
	H-24	" 537	2-25	3.67	1.41	0.47	0.732	99.0	0.652	97.9
	H-25	" 536	3-10	3.66	1.60	0.59	0.750	98.4	0.652	98.3
IV	H-20	DWEPK 791	2-9	5.73	1.57	1.15	1.068	99.3	0.846	100.0
	H-26	" 789	3-17	3.65	1.60	1.03	1.056	100.3	0.852	100.2
	H-29	" 785	3-31	3.67	1.61	0.835	1.064	99.9	0.837	99.9
V	H-27	DWEPK 788	3-20	3.71	1.63	0.70	1.051	100.2	0.906	99.6
	H-28	" 787	3-24	3.64	1.60	0.96	1.060	100.1	0.895	98.9

the maximum cohesion was assumed to be kept constant for the specimens of a test series by keeping initial soil structure, $\bar{\sigma}_1$, the plane of $\bar{\sigma}_1$ (horizontal), and void ratio constant within the series. The degree of anisotropy of the soil structure was varied by changing the $\bar{\sigma}_1/\bar{\sigma}_3$ ratio to which the specimens were consolidated prior to CFS-testing. This ratio was varied from 1.0 to 1.6 and it is assumed that significant variation in structural anisotropy was produced. Comparison of the results of such tests were then used to judge the possible anisotropic behavior of the cohesion component of soil strength.

Scope.—Table 1 summarizes the scope of this investigation. In this investigation two machine-remolded, near-saturated clays were used. Kolinite was chosen as the main clay because previous research³ showed it had strength properties similar to a variety of clays of natural composition and had advantages of (a) additional structural sensitivity, in spite of machine remolding, (b) known mineralogy, and (c) relatively high permeability which aids the convenience of CFS-testing. Four of the five series used duplicate specimens of koalinite so that these series may be compared directly. To evaluate possible effects of mineralogy and grain size distribution, Series III was performed in an identical manner to Series II except that Boston blue clay was used. This is an illite-type clay with considerable silt. It is important to note that both kaolinite and illite are platy clay minerals and the results presented herein may be limited to clays with similar type clay minerals.

Series I and II are duplicates, except that the stresses in II are approximately double those of I. The stress was doubled to determine whether the magnitude of stress was a significant variable. The values of 1.80 kg per sq cm and 3.65 kg per sq cm were chosen for convenience. The ratio $(\bar{\sigma}_1/\bar{\sigma}_3)_c$ was limited to 1.6 because of excessive compressive strain encountered at higher values. Series IV was included to evaluate possible influences of the technique used to obtain the non-hydrostatic consolidation.

Table 2 presents additional detail about test and specimen conditions.

TESTING PROCEDURES

Equipment Used.—The triaxial and anisotropic loading equipment used was developed by the Norwegian Geotechnical Institute. A complete description of the equipment shown in Fig. 2 is available.⁵ The NGI cell piston design was modified to accommodate a 1/4-in. piston running in ball-bearing sleeves.⁶

An SR-4 load cell was developed to replace the use of a proving ring. This cell has a compression of 0.006 mm per kg versus 0.090 mm per kg for a proving ring of the same load capacity (30 kg). This increase in rigidity enabled the tests to be run at a more constant rate of strain. The design of the load cell is reported elsewhere.⁷

⁵ "Triaxial Equipment Developed at the Norwegian Geotechnical Institute," by A. Andresen, J. Bjerrum, E. DiBiago, and B. Kjaernsli, Norwegian Geotech. Inst. Publications No. 21, Oslo, 1957.

⁶ "Prestress induced in Consolidated-Quick Triaxial Tests," by A. Casagrande and S. D. Wilson, *Proceedings, 3d Internatl. Conf. on Soil Mechanics and Foundation Engrg., Switzerland, 1953, Vol. 1, p. 106.*

⁷ "An Experimental Study of the Effect of Anisotropical Consolidation on the Cohesion and Friction in Saturated Clay," by J. R. Hall, Jr., thesis presented to the Univ. of Florida, at Gainesville, Fla., in June, 1960, in partial fulfillment of the requirements for the degree of Master of Science.

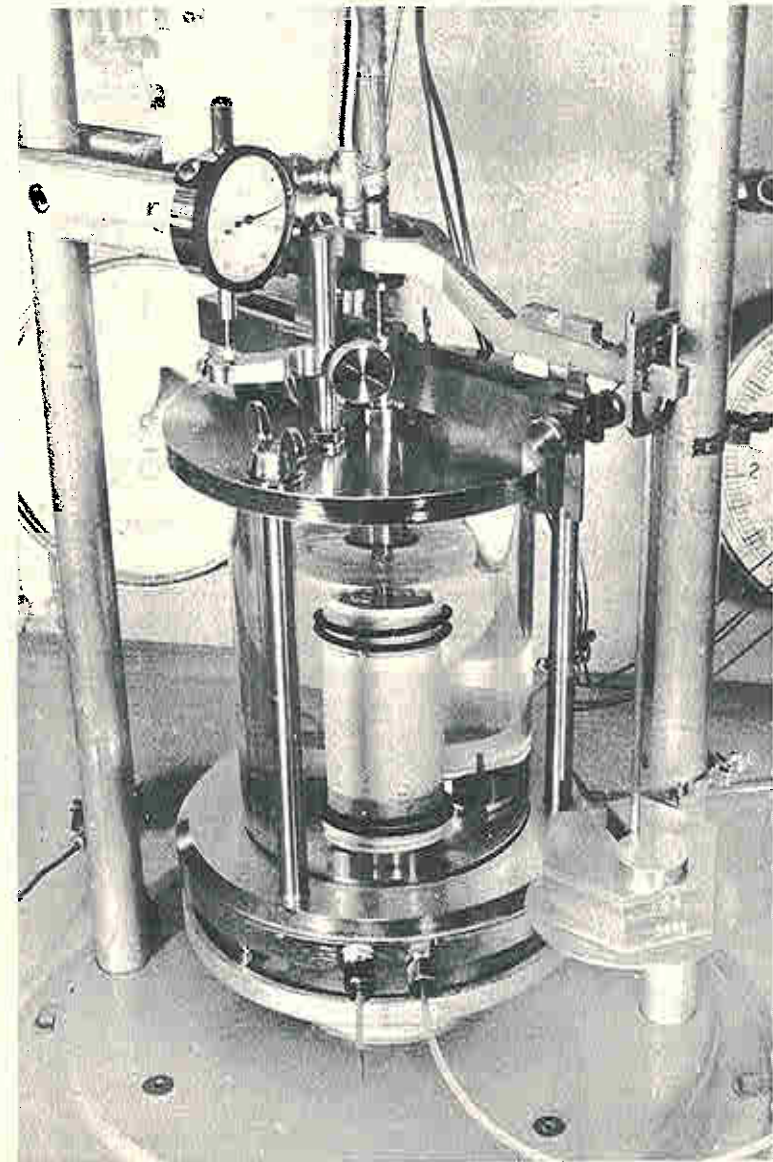


FIG. 2.—SPECIMEN DURING CFS-TEST AFTER ANISOTROPIC CONSOLIDATION

For preparation of duplicate remolded specimens with a high degree of saturation and structural duplication, a "Vac-Aire" extruder was used.⁸ A helical particle-alignment structure results from the use of this extruder, and this, unfortunately, complicates the mental picture of the structural effect of subsequent non-hydrostatic consolidation. However, non-hydrostatic consolidation should develop some degree of anisotropic structure when compared to the starting condition.

Specimen Preparation.—The initial dimensions of all specimens were 8.00 cm high and 3.59 cm in diameter. Two clays were used. Table 3 lists the Atterberg limits, specific gravity, and grain size analyses of both.

Kolinite.—The kaolinite specimens were prepared from "as received" kaolinite powder. This was a particularly pure commercial kaolinite. The powder was mixed with distilled water to give a water content between 40% and 41%. A detailed description of this clay and a study of its geologic origin is available.⁹ These specimens were designated DWEPK.

Boston Blue Clay.—The Boston blue clay was obtained from a pit in Cambridge, Mass. In remolding, the clay had to be allowed to partially dry in order to gain sufficient strength for extrusion into round bars. It was finally extruded at a water content of 26%. These specimens were designated BBC.

TABLE 3.—CLAY PROPERTIES

Clay	Liquid Limit, in %	Plasticity Index, in %	G used in calculations	Percentage Finer Than		
				200 sieve	50 μ	2 μ
DWEPK	52	21	2,609	100	100	60
BBC	38	19	2,810	98	87	53

Internal wool drains, together with filter paper strips along the sides and filter paper caps on the top and bottom, were used in triaxial tests. The specimens were sealed from the cell pressure media (water) with two latex membranes (each 0.056 mm thick) separated by a layer of grease. Further details concerning the preparation procedure are available.³

Testing Procedures.—

Non-hydrostatic Consolidation.—In order to reduce the void ratio variation within a test series, the tests were run so that the only variable was the minor principal stress applied during consolidation. The major principal stress applied during consolidation was held nearly constant within each series, giving essentially the same void ratio after consolidation in spite of the greatly different $(\bar{\sigma}_1/\bar{\sigma}_3)_c$ values of 1.0, 1.2, 1.4, and 1.6 (Table 2). With e and $\bar{\sigma}_1$ constant after consolidation, the effect of the non-hydrostatic consolidation could be better evaluated.

The method used for consolidating the specimens in Series I, II, III and IV, which is referred to as standard in Table 1, was as follows: Using the aniso-

⁸ "De-Aired, Extruded Soil Specimens for Research and for Evaluation of Test Procedures," by H. Matlock, Jr., C. W. Fenske, and R. F. Dawson, A.S.T.M. Bulletin No. 177, October, 1951.

⁹ "Kaolinitic Sediments in Peninsular Florida and Origin of the Kaolin," by E. C. Pirkle, Economic Geology, Vol. 55, No. 7, November, 1960, p. 1382.

tropic loading device, the weights are suspended on a hanger which transmits the load to the piston of the triaxial cell through a system of knife edge supports with a lever-arm ratio of 5 (Fig. 2). The load to the piston is five times the load applied to the hanger. After noting the characteristic shape of the semi-log plot of the time-consolidation curves for kaolinite under a hydrostatic pressure of 3.65 kg per sq cm, it was observed that at approximately 6 ml decrease of volume, as measured by the amount of water drained from the specimen into a burette, the consolidation curve starts the turn into secondary consolidation. The total volume change was slightly more than 7 ml. It was decided to add the weights at equal intervals of volume change and to have all of the weights added by the end of 6 ml or 6/7 of the total consolidation. The weight increments used were determined by the convenience of the size of weights available. This load increment was usually 1 kg on the specimen, and from four to eleven increments were applied during the approximately 25 min required to consolidate 6 ml. The cell pressure was applied in one step at the beginning of consolidation and remained constant throughout the piston loading cycle. A similar procedure was used for the BBC in Series III and the kaolinite at $\bar{\sigma}_1 = 1.80$ kg per sq cm in Series I.

All of the anisotropic load was not added at the beginning of consolidation because the specimen was not able to support the total load without excessive strain or possible failure. By adding the load after equal increments of volume change, the specimen was given time to consolidate and thereby increase strength to support the following load increment without obviously excessive strain.

Two other methods of consolidation were used in Series V. For test H-27 the specimen was first consolidated hydrostatically under a pressure of 2.28 kg per sq cm. After the consolidation had proceeded 1,370 min in the secondary stage, following an approximate 50 min primary, the axial load was then applied in increments until the maximum stress, $\bar{\sigma}_1$, was equal to 3.71 kg per sq cm. In test H-28 the axial load and cell pressure were both increased in six increments such that the stress ratio $\bar{\sigma}_1/\bar{\sigma}_3$ was equal to 1.6 at all times. The specimen was allowed to consolidate for 8 hr between each increment. The final stresses on the specimen after consolidation were $\bar{\sigma}_1 = 3.64$ kg per sq cm and $\bar{\sigma}_3 = 2.28$ kg per sq cm.

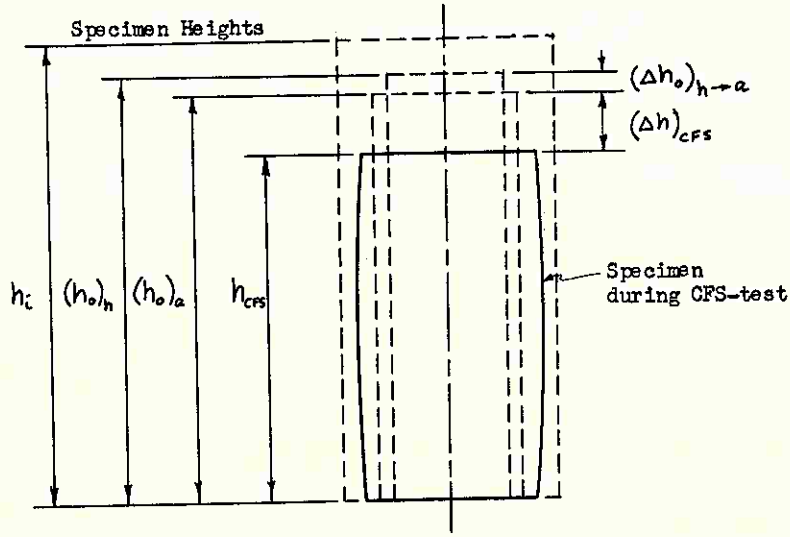
In all tests for Series I, II, and III the time allowed for secondary consolidation after the final consolidation load increment varied between 17.4 hr and 19.7 hr.

Strength Testing.—As mentioned in the Introduction, the CFS-test was used for determining cohesion and friction as a function of strain. The compression rate of 0.0053 mm per min (0.0002 in. per min) was chosen the same for all tests. This rate permitted obtaining the required data for computing cohesion and friction over the range of approximately 1/2% to 5% axial strain within a compression period of approximately 12 hr.

COHESION AND FRICTION

After non-hydrostatic consolidation the specimen is supporting a deviator stress,

$$\sigma_a = \sigma_1 - \sigma_3 \dots \dots \dots (4)$$



LEGEND

- h_i = initial extruded height
- $(h_o)_h$ = height after hydrostatic consolidation to $(\bar{\sigma}_1)_c$
- $(h_o)_a$ = height after non-hydrostatic consolidation to same $\bar{\sigma}_1$; start of CFS-test
- h_{CFS} = height during CFS-test

STRAINS

$$\frac{(\Delta h)_{h \rightarrow a}}{(h_o)_a} = \text{axial strain during non-hydrostatic consolidation} = \epsilon_a$$

$$\frac{(\Delta h)_{CFS}}{(h_o)_a} = \text{axial strain due to CFS-test} = \epsilon_{CFS}$$

$$\text{Total strain} = \epsilon = \frac{(\Delta h)_{h \rightarrow a} + \Delta h_{CFS}}{(h_o)_h} \approx \epsilon_a + \epsilon_{CFS}$$

FIG. 3.—DEFINITION OF SPECIMEN STRAINS

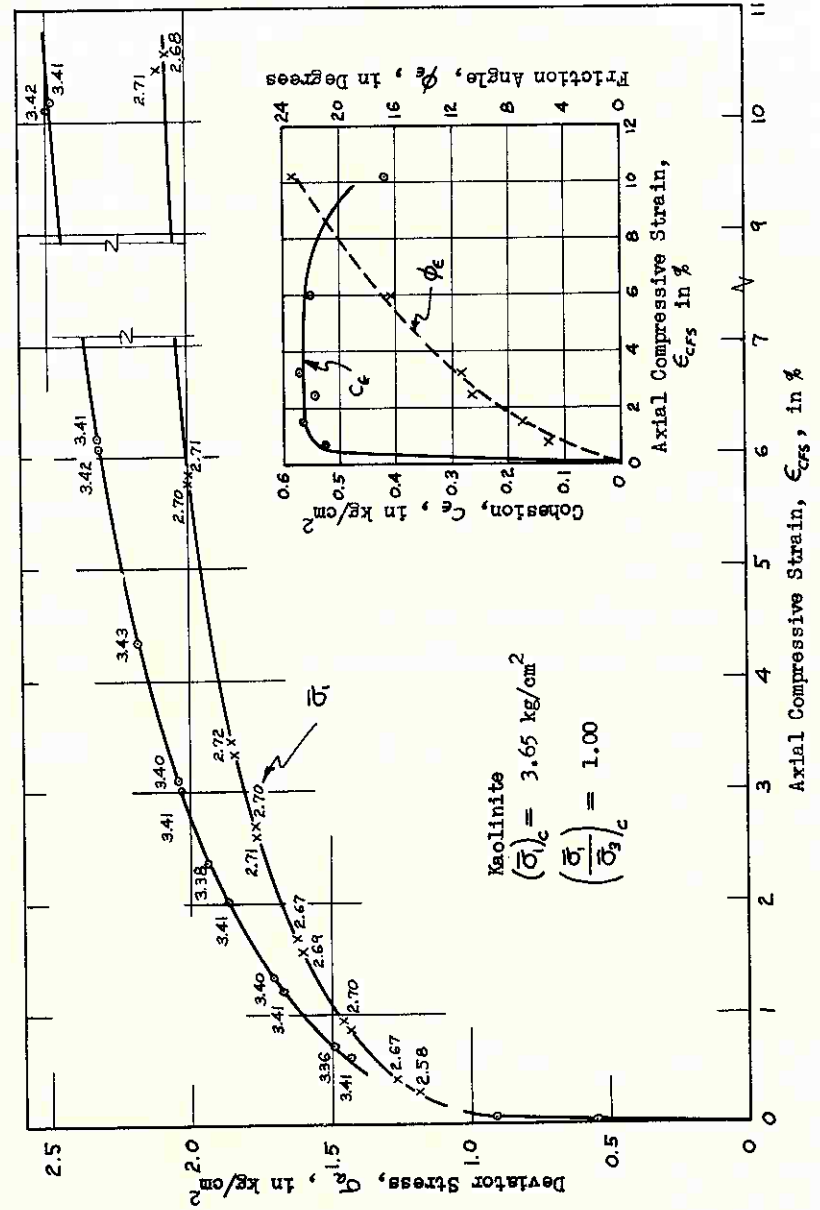


FIG. 4.—STRESS-STRAIN CURVES AND COMPUTED RESULTS FOR TEST H-13, SERIES II

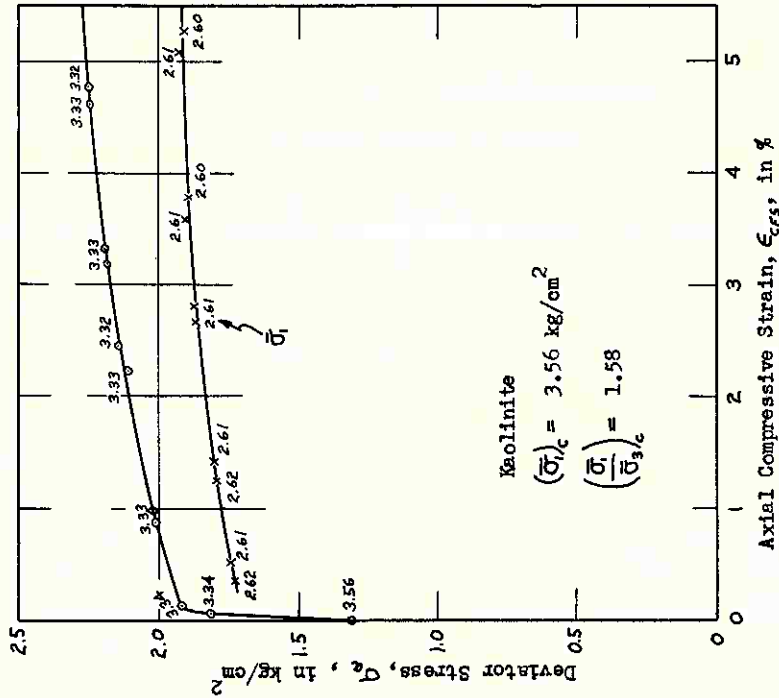
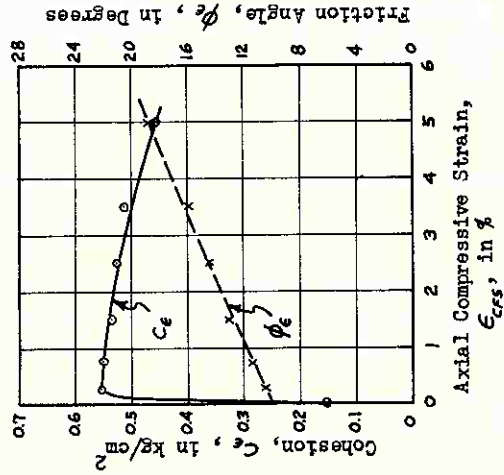


FIG. 7.—STRESS-STRAIN CURVES AND COMPUTED RESULTS FOR TEST H-16, SERIES II



and has undergone axial strain as shown in Fig. 3. In order to support this deviator stress, the values of cohesion and friction cannot both be zero. If the

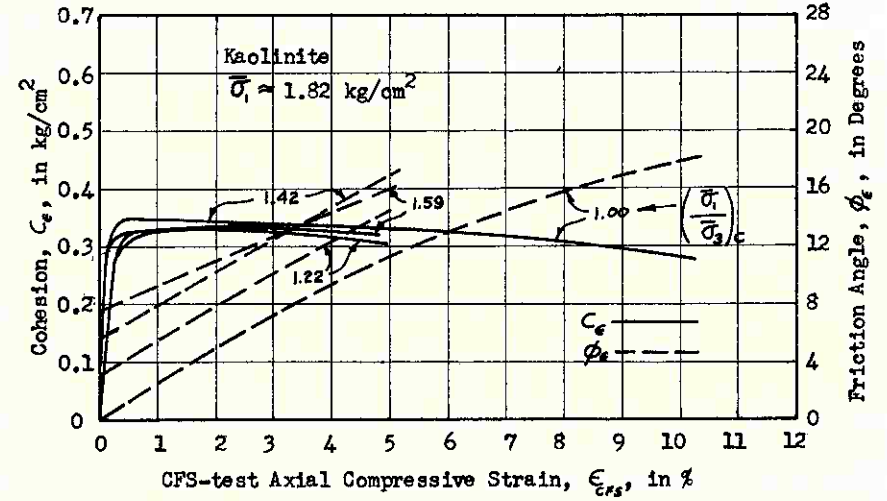


FIG. 8.—VARIATION OF COHESION AND FRICTION WITH CFS-TEST STRAIN FOR SERIES I

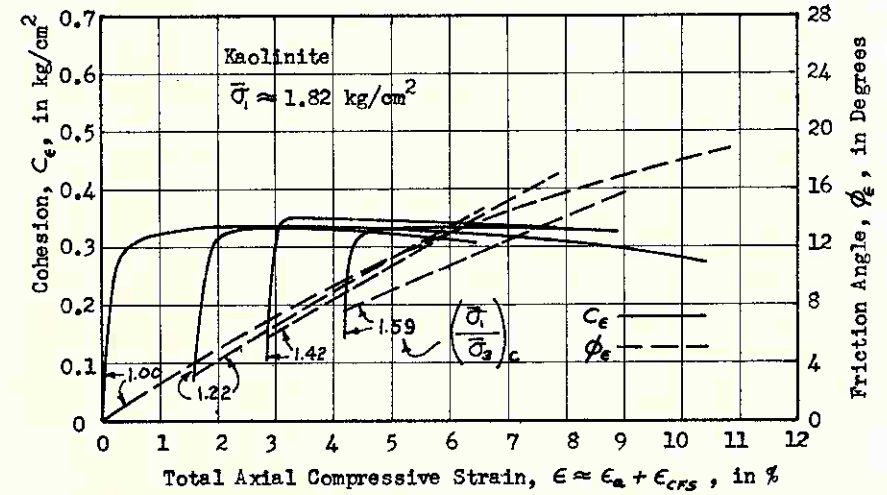


FIG. 9.—VARIATION OF COHESION AND FRICTION WITH TOTAL STRAIN FOR SERIES I

specimen is subjected to a hydrostatic state of stress, as in the case of hydrostatic consolidation, then at zero CFS-test strain both the cohesion and friction were assumed to be zero.

For the non-hydrostatic case, the following method was used to compute the values of cohesion and friction at zero CFS-test strain: The values of cohesion and friction are computed only at strains where the two required $\bar{\sigma}_1$ curves are

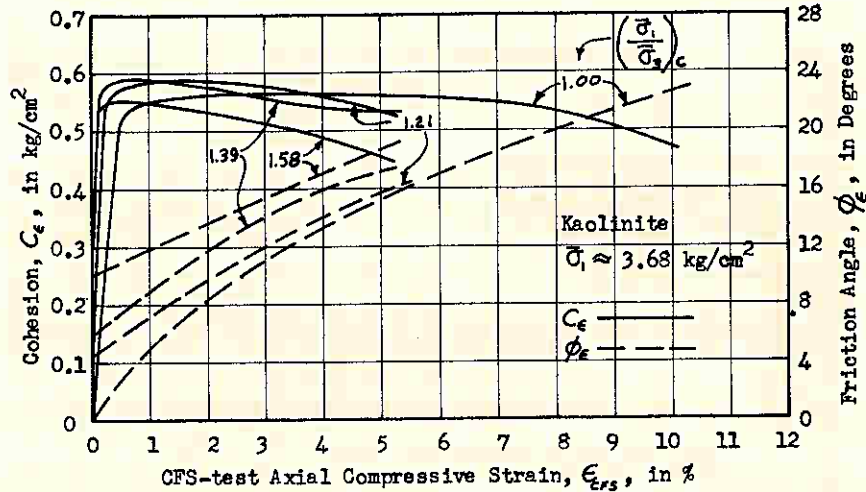


FIG. 10.—VARIATION OF COHESION AND FRICTION WITH CFS-TEST STRAIN FOR SERIES II

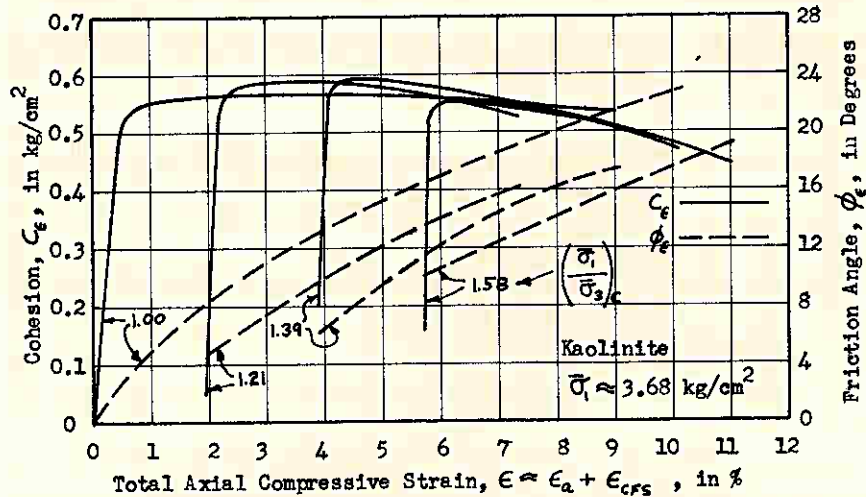


FIG. 11.—VARIATION OF COHESION AND FRICTION WITH TOTAL STRAIN FOR SERIES II

fully defined and c_ϵ and ϕ_ϵ are plotted against that strain. This may be seen in Figs. 4, 5, 6, and 7, that present the detailed results for Series II. Because it is impossible, from the data obtained, to draw the two curves for different ef-

fective stresses at small values of CFS-test strain (less than 0.25%), an extrapolation procedure was used. The extensive testing experience with DWEPK and BBC specimens hydrostatically consolidated for approximately 23 hr prior

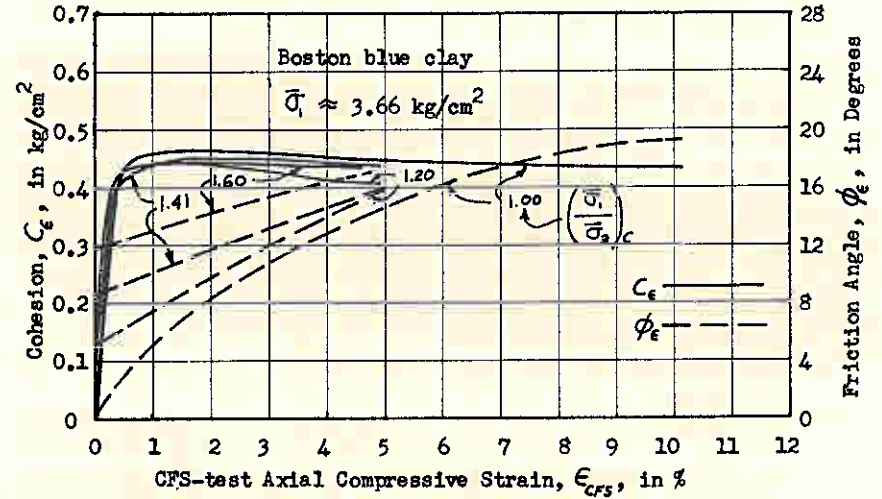


FIG. 12.—VARIATION OF COHESION AND FRICTION WITH CFS-TEST STRAIN FOR SERIES III

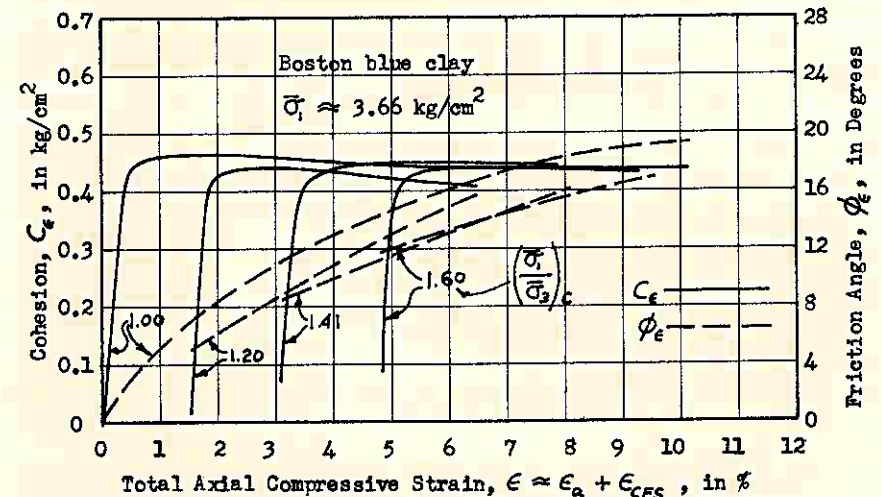


FIG. 13.—VARIATION OF COHESION AND FRICTION WITH TOTAL STRAIN FOR SERIES III

to shear testing indicated that at CFS-test strains of less than 1% the frictional component of strength varies much less rapidly with strain than the cohesion.³ Thus, the friction was extrapolated to zero strain instead of the cohesion. This

value of friction was assumed to be the value at zero CFS-test strain and was used to compute the value of cohesion at zero strain by using Eq. 3. The initial values of cohesion and friction as computed by this method are shown on the curves plotted for the individual test (Figs. 4 to 7) as well as the curves showing each complete series (Figs. 8 to 13).

Series I, II, and III.—Series I, II, and III were performed in the same manner and are therefore presented together. This analysis began with a review of the strain history of each specimen, as shown in Fig. 3. After the initial extrusion the specimen was consolidated with $(\bar{\sigma}_1/\bar{\sigma}_3)_c$ ratios up to 1.6. The application of a deviator stress during consolidation resulted in axial compression greater than the height reduction measured during hydrostatic consolidation to the same value of $\bar{\sigma}_1$. This additional strain is designated ϵ_a . Then a strain ϵ_{CFS} was imposed during the CFS-test. Although the foregoing two strains were computed with a different reference height than the total strain ϵ , the percentage difference in the heights $(h_o)_a$ and $(h_o)_h$ is small and it is considered adequate to estimate the total strain due to deviator stress as

$$\epsilon = \epsilon_a + \epsilon_{CFS} \dots \dots \dots (5)$$

The cohesion-friction-strain curves for these series are presented in Figs. 8 to 13. Two strain coordinates are used. Figs. 8, 10, and 12 are based on the CFS-test strain, ϵ_{CFS} ; Figs. 9, 11, and 13 on the estimated total deviator strain ϵ . From both these sets of figures it may be seen that the cohesion behavior is a function of $(\bar{\sigma}_1)_c$ and is unaffected by $(\bar{\sigma}_3)_c$. Thus, these results support the concept that cohesion is an isotropic property.

Considering only Figs. 8, 10, and 12, it appears that the friction-strain behavior was progressively displaced toward higher friction values with increasing values of $(\sigma_1/\sigma_3)_c$. However, these figures do not account for the deviator strain that occurred during the non-hydrostatic consolidation. When plotted on the basis of the estimated total strain, as in Figs. 9, 11, and 13, there is some displacement toward lower friction values with increasing $(\bar{\sigma}_1/\bar{\sigma}_3)_c$, but that the general friction-strain behavior is similar to that of the hydrostatically consolidated specimen. The values used for ϵ_a are critical in the foregoing comparison and it should be realized that the step-loading procedure used to apply the deviator stress during consolidation complicates the estimate of ϵ_a . The estimate used herein, as shown in Fig. 3, is probably not sufficiently refined to permit a conclusion regarding any displacement effect of non-hydrostatic consolidation on friction-strain behavior.

A conclusion is also not possible with regard to another important aspect of friction behavior, pore pressure development. Pore pressure is controlled in the CFS-test and thus its development in response to other factors possibly associated with non-hydrostatic consolidation was not considered in this research program.

Series IV.—Three tests were run to determine the effect of the length of time permitted for non-hydrostatic consolidation on the kaolinite. The three tests showed no important differences in their results. When the value of friction was extrapolated to zero CFS-test strain to compute cohesion at this strain, the computed value of cohesion ranged from -0.08 kg per sq cm to 0.00 kg per sq cm. The value of friction was then mathematically adjusted to suit a cohesion of zero.

The three Series IV tests were allowed to stand for 66 hr, 131 hr, and 299 hr, respectively, after the completion of primary consolidation. From the re-

sults of the Series IV and previous tests it was concluded that as the non-hydrostatically loaded specimen continues to consolidate in the secondary stage the deviator stress is initially carried by both cohesion and friction but is eventually carried totally by friction as the cohesion drops to zero. However, a zero cohesion is only possible for soils able to develop the required friction to carry the total load.

The conclusion of the cohesion to friction transfer is strongly supported by the unpublished experimental work of R. G. Bea,¹⁰ A. M. ASCE, and his im-

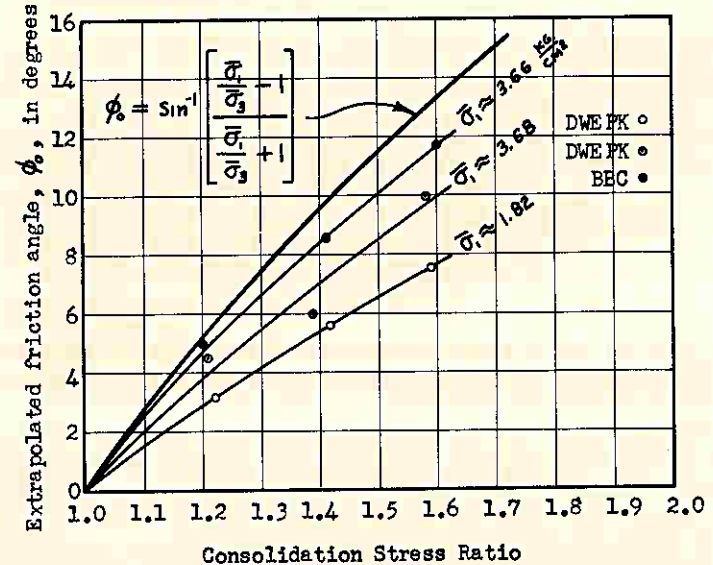


FIG. 14.—FRICTION ANGLE AT ZERO CFS-TEST STRAIN VERSUS CONSOLIDATION STRESS RATIO

portant contribution to its recognition is acknowledged. The present work on this subject is preliminary. Extensive additional research is in progress.

The tests in Series I, II, and III were conducted after secondary consolidation times between 17.4 hr and 19.7 hr. This was insufficient time for the cohesion to drop to zero, as seen in Figs. 9, 11, and 13. The value of friction angle at zero CFS-test strain, ϕ_0 , versus consolidation stress is plotted in Fig. 14 for test Series I, II, and III, together with the curve representing the value

¹⁰ "An Experimental Study of Cohesion and Friction During Creep in Saturated Clay," by R. G. Bea, thesis presented to Univ. of Florida, Gainesville, Fla., in June, 1960, in partial fulfillment of the requirements for the degree of Master of Science.

of friction that would be obtained had the specimen consolidated over an adequate length of time for the cohesion to drop to zero. If cohesion is equal to zero, then it follows from Eq. 3 that

$$\phi_0 = \sin^{-1} \left[\frac{\frac{\bar{\sigma}_1}{\bar{\sigma}_3} - 1}{\frac{\bar{\sigma}_1}{\bar{\sigma}_3} + 1} \right] \dots \dots \dots (6)$$

The required time for the cohesion to drop to zero seemed to depend on $\bar{\sigma}_1$ as well as the type of clay. The BBC transferred cohesion to friction more rapidly than DWEPK, and the DWEPK at $\bar{\sigma}_1 = 3.65$ kg per sq cm more rapidly than the same clay at $\bar{\sigma}_1 = 1.80$ kg per sq cm.

Series V.—Tests H-27 and H-28 were consolidated as described under the heading "Testing Procedures" to determine the effect of the loading method used to arrive at the final principal stresses applied during consolidation. There was no significant difference between the results computed from these tests and the comparable tests of Series II which used the standard method. Considering the differences in the loading method used to consolidate the specimens it was concluded that the method of consolidation had no effect on the cohesion and friction of the kaolinite tested. However, it must be noted that the time allowed for secondary consolidation after the application of the last consolidation load increment was about the same for all tests compared.

CONCLUSIONS

The following is a summary of the conclusions in regard to non-hydrostatic consolidation and its affect on the cohesion and friction for the clays and experimental conditions of this study.

1. The anisotropic soil structure assumed to result from non-hydrostatic consolidation did not affect subsequent cohesion-strain behavior. This behavior also seems independent of the consolidation procedure when equal secondary consolidation times are used. The results suggest that cohesion is an isotropic property in the two platy clay mineral soils tested.

2. The value of friction at zero CFS-test strain, after approximately equal consolidation conditions, is increased by an increase of consolidation stress ratio, $(\bar{\sigma}_1/\bar{\sigma}_3)_c$. However, the variation of friction with strain is similar to that of a hydrostatically consolidated specimen.

3. During non-hydrostatic consolidation the deviator stress is carried at first by cohesion and friction but cohesion reduces and eventually drops to zero if the soil has adequate friction capability.

ACKNOWLEDGMENTS

The writers are pleased to thank the Engineering Sciences Division of the National Science Foundation, the Engineering and Industrial Experiment Station and the Graduate School of the University of Florida for their financial support of this research. F. E. Richart, Jr., F. ASCE, and W. H. Zimpfer, M. ASCE, of the Civil Engineering Department of the University of Florida contributed thoughtful reviews of the original manuscript.

APPENDIX.—NOTATION

The following symbols have been adopted for use in the paper.

c_ϵ	= cohesion at strain ϵ ;
e	= void ratio;
G	= specific gravity of soil solids;
h_i	= initial extruded height of specimen (Fig. 3);
h_{CFS}	= specimen height during CFS-test (Fig. 3);
$(h_0)_a$	= specimen height after non-hydrostatic consolidation; start of CFS-test (Fig. 3);
$(h_0)_h$	= specimen height after hydrostatic consolidation (Fig. 3);
S	= degree of saturation;
u	= excess hydrostatic pore water pressure;
ϵ	= axial compressive strain (Fig. 3);
ϵ_a	= axial compressive strain during non-hydrostatic consolidation (Fig. 3);
ϵ_{CFS}	= axial compressive strain due to CFS-test (Fig. 3);
μ	= micron, 0.001 mm;
$\bar{\sigma}$	= effective normal stress;
σ_1	= major principal stress (horizontal plane);
$\bar{\sigma}_1$	= effective major principal stress;
$(\bar{\sigma}_1)_c$	= effective major principal stress developed during consolidation;
$(\bar{\sigma}_1)_{high}$	= higher valued $\bar{\sigma}_1$ curve during CFS-test (Fig. 1);
$(\bar{\sigma}_1)_{low}$	= lower valued $\bar{\sigma}_1$ curve during CFS-test (Fig. 1);
σ_3	= minor principal stress (vertical plane);
$\bar{\sigma}_3$	= effective minor principal stress;
$(\bar{\sigma}_3)_c$	= effective minor principal stress developed during consolidation;
$\left(\frac{\bar{\sigma}_1}{\bar{\sigma}_3}\right)_c$	= consolidation stress ratio, effective after primary consolidation;
σ_a	= deviator stress = $(\sigma_1 - \sigma_3)$, applied through vertical piston;
σ_h	= hydrostatic stress in triaxial cell;
\bar{T}	= shear stress;
\bar{T}_ϕ	= shear stress on plane of maximum stress obliquity for frictional component of strength;
ϕ_0	= angle of internal friction developed at start of CFS-test ($\epsilon_{CFS} = 0$); and
ϕ_ϵ	= angle of internal friction at strain ϵ .